Metal-insulator transition temperature enhancement in $La_{0.7}Ca_{0.3}MnO_3$ thin films

M. Salvato,[a] A. Vecchione, A. De Santis, F. Bobba, and A. M. Cucolo
Dipartimento di Fisica "E.R. Caianiello," Università degli Studi di Salerno and Instituto Nazionale per la Fisica della Materia (INFM) Laboratorio Regionale SUPERMAT, via S. Allende I-84081, Baronissi, Salerno, Italy

(Received 3 August 2004; accepted 7 March 2005; published online 4 May 2005)

The effect of oxygen annealing on the structural and transport properties of $La_{0.7}Ca_{0.3}MnO_3$ thin films deposited on $SrTiO_3$ substrates has been investigated by x-ray diffraction analysis and resistive measurements. The as-grown films are fully tensile strained on the substrates and show a depressed metal-insulator transition temperature $T_p = 131$ K. As the oxygen content is increased due to longer annealing times, significantly higher T_p are measured, up to 247 K. Correspondingly, an increase of the out-of-plane lattice parameter is observed while the in-plane lattice constants do not change with respect to the as-grown films, which prevents any interpretation of a T_p dependence on the strain. The large increase in T_p is then interpreted in terms of a combined effect of the Mn^{4+}/Mn^{3+} ratio variation, the change in the carrier density in the *a-b* planes, and the increase in the hydrostatic strain with the oxygen annealing. © *2005 American Institute of Physics*. [DOI: 10.1063/1.1898451]

I. INTRODUCTION

$La_{1-x}A_xMnO_3$ manganite compounds, with *A* being a divalent alkali ion such as Ca^{2+}, Sr^{2+}, or Ba^{2+}, have recently attracted great theoretical and experimental interest because of their unusual charge-transport dynamics and their outstanding magnetic properties.[1,2] Indeed these materials show both metal-insulator and paramagnetic-ferromagnetic transitions with colossal magnetoresistance (CMR) effects for concentrations $0.2 \lesssim x \lesssim 0.5$.[3,4] Recently, much attention has been devoted to the transport properties of manganite thin films, because of their potential applications in devices such as magnetic reading heads, field sensors, and memories. Apart from the technological applications, manganite thin films present other interesting properties quite different from the related bulk compounds. In particular, both the metal-insulator transition temperature T_p and the paramagnetic-ferromagnetic transition temperature T_c are strongly affected by many parameters such as film thickness,[5–8] lattice strain,[9–15] and substrate-induced depletion layers.[16] Both T_p and T_c take approximately the same values observed in the case of bulk samples only for thickness greater than about 1000 Å,[17] while very different values are observed in films of thickness less than 500 Å.[5] Moreover, for $La_{1-x}Ca_xMnO_3$ films deposited on $SrTiO_3$ (STO) substrates, a tensile in-plane strain is found, which results in lower T_p and T_c, whereas an increase of these temperatures is observed for the films deposited on $LaAlO_3$ (LAO) where a compressive in-plane strain is present.[18,19] Oxygen concentration also plays an important role in the variation of the Mn–O–Mn bond angles and of the Mn^{4+}/Mn^{3+} ratio that both affect the mechanism of the charge transport due to the presence of itinerant electrons in the e_g valence bands.[7,19,20] One of the advantages of studying thin films is that these phenomena can be, at least in principle, studied separately. The effect of the strain on the transport properties can be investigated by depositing the same material on different substrates, while fabrication of films with different thicknesses on the same substrates can give information on the thickness dependence of the transport properties. In order to study the effect of the oxygen content on the transport properties of $La_{0.7}Ca_{0.3}MnO_3$ (LCMO) thin films, we deposited a number of samples with the same thickness on STO substrates and we annealed them in oxygen at the same temperature for different times. A large enhancement of T_p is observed for increasing annealing times while the in-plane lattice parameters remain unchanged. We attribute these findings to the Mn^{4+}/Mn^{3+} ratio variation, to the change in the carrier density in the *a-b* planes, and to the increase in the hydrostatic strain, all effects resulting from the oxygen incorporation in the crystal structure.

II. SAMPLES PREPARATION AND EXPERIMENTAL RESULTS

$La_{0.7}Ca_{0.3}MnO_3$ thin films with a nominal thickness of 300 Å have been deposited on STO (001)-oriented substrates by a dc-sputtering technique in high oxygen pressure from a stoichiometric target. The as-grown samples studied in this paper were deposited at an oxygen partial pressure of 3.0 mbar and at a substrate temperature of 900 °C.[21] These conditions guarantee a high reproducibility of the structural and transport properties. After deposition, some of the films underwent *ex situ* annealing treatments for different times in a controlled oxygen flux of 20 l/h at a temperature of 900 °C. Energy dispersive spectroscopy (EDS) measurements pointed out that the cation concentrations were unchanged with the oxygen annealing and that the target stoichiometry was preserved in the films. The experimental results we report on are representative of the properties of as-grown films (LCM1) and of annealed films LCM2 and LCM3, treated for 1 and 3 h, respectively.

[a]Electronic mail: salvato@sa.infn.it

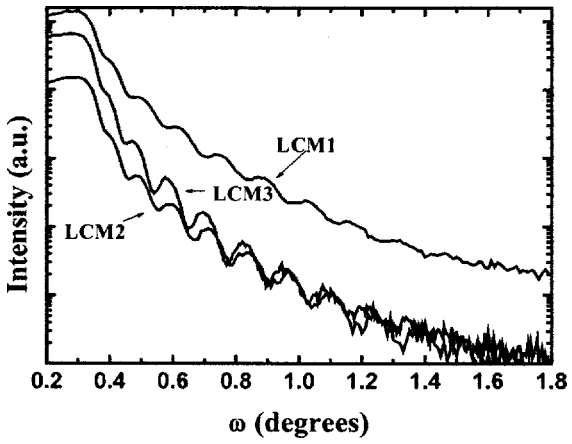

FIG. 1. Reflectivity spectra of the as-grown film (LCM1) and of the two oxygen-annealed films (LCM2 and LCM3).

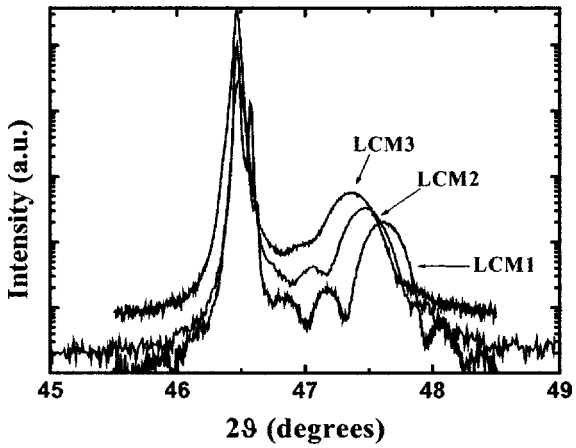

FIG. 2. $\vartheta-2\vartheta$ spectra of the three samples of Fig. 1 around the (002) peaks of the substrates ($2\vartheta=46.464$) and films. The shift of the film reflections corresponds to the decrease in the *c* axis with the oxygen content.

The transport properties were studied by resistivity versus temperature measurements in the range from 77 to 300 K. The structural studies were carried out by x-ray reflectivity and diffraction measurements using a Philips X-Pert MRD diffractometer. Monochromatic Cu $K\alpha_1$ radiation was obtained equipping the diffractometer with a four-crystal Ge (220) asymmetric monochromator and a graded parabolic mirror positioned on the primary arm which also reduces the incident beam divergence to 0.12 arc sec. A parallel beam collimator was positioned between the sample and the detector in the case of reflectivity measurements. The structural data are discussed by assuming a cubic structure of bulk LCMO with unit-cell parameter $a_B=b_B=c_B=3.859$ Å and a cubic perovskite structure for the STO substrates with $a_S=3.905$ Å.

The thickness of the samples was measured from the separation between the interference fringes of the reflectivity spectra shown in Fig. 1. In agreement with the expected thickness, as estimated from the deposition time, a value of 320 Å has been obtained.

Moreover, the difference between the amplitude of the fringes of the as-grown and the two annealed films is evident. The lower the amplitude of the interference fringes, the higher is the surface roughness. This is supported by the theoretical fittings of the experimental data performed by using the Parrat[22] and Nevot–Croce[23] formalism with the surface roughness as the free parameter. The estimated values correspond to 4 Å for the as-grown LCM1 sample and to 2 Å in the case of both the oxygenated films. The reflectivity data can be interpreted assuming that the oxygen postannealing produces smoother surfaces with reduced roughness. Through the same procedure we evaluate a density of about 6 g/cm^3 for all the samples.

The $\vartheta-2\vartheta$ measurements (not reported) performed in the range $5°<2\vartheta<120°$ on the as-grown and postannealed films showed that these were oriented with the (001) planes parallel to the substrate surface and no presence of spurious phases was revealed. The $\vartheta-2\vartheta$ scans of the (002) reflection of the as-grown and the oxygen annealed films are reported in Fig. 2. For all the samples, the substrate peaks coincide in the 2ϑ value and can be considered as a reference for the peak position measurements of the films. The inferred *c*-axis values are reported in Table I. We observe that these are lower than the bulk value and increase for longer oxygen annealing times, thus providing evidence of an increase of the separation between the (001) planes with the oxygen content. The presence of the satellites fringes in the as-grown film spectrum is an indication of the good crystal quality of this sample. Moreover, the position of the satellite peaks gives a value of the sample thickness which is in good agreement with that obtained by reflectivity measurements. Interestingly, this indicates that the separation among the (001) planes is constant along the whole film thickness, suggesting that no dead layer is present in our as-grown films.

Comparing the reported spectra in Fig. 2, a progressive smoothing of the satellite peaks for increasing oxygen content is observed. The structural disorder is so enhanced by the oxygen insertion in the atomic lattice and a further confirmation is obtained by the increased values of the full width at half maximum (FWHM) (reported in Table I) of the rocking curves shown in Fig. 3. These values correspond to a lateral structural coherency of about 2000 Å for the as-grown film and of about 500 Å for the fully oxygenated sample, suggesting that the effect of the oxygen is to enhance the mosaicity of the crystal structure.

TABLE I. T_p=metal-insulator transition temperature; c_F=out-of-plane film axis; a_F, b_F=in-plane film axes, FWHM=full width at half maximum of the rocking curves shown in Fig. 3; $\varepsilon_B=2\varepsilon_{100}+\varepsilon_{001}$ (hydrostatic strain); $\varepsilon_{JT}=(2/3)^{1/2}(\varepsilon_{001}-\varepsilon_{100})$ (biaxial strain); $\varepsilon_{001}=(c_F-c_B)/c_B$, $\varepsilon_{100}=(a_F-a_B)/a_B$.

Sample	c_F(Å)	a_F(Å)	FWHM rocking (°)	T_p(K)	ε_B	ε_{JT}	$\varepsilon_B/\varepsilon_{JT}$
LCM1	3.816	3.91	0.049	131	0.0101	0.0177	0.57
LCM2	3.827	3.90	0.070	232	0.0129	0.0154	0.84
LCM3	3.835	3.90	0.132	247	0.0150	0.0137	1.10

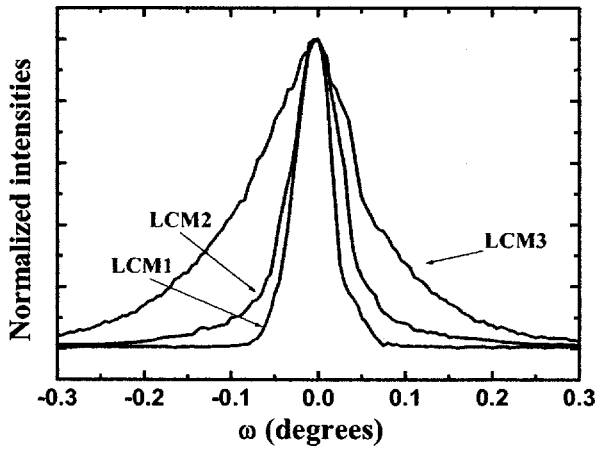

FIG. 3. Rocking curves of the three studied samples. The FWHM (reported in Table I) increase with the oxygen annealing.

The reflectivity and the structural measurements indicate that the annealing procedure leads to a reduction of the surface roughness and, at the same time, to an increase of the atomic disorder in the lattice. We explain these results assuming that the high annealing temperature enhances the lateral diffusivity of the deposited material, thus reducing the surface roughness, whereas the oxygen incorporation is responsible for some atomic disorder.

In order to investigate the in-plane lattice matching between film and substrate, reciprocal space maps have been measured on asymmetric reflections. The reciprocal space maps containing the (013) reflections of both the film and the substrate are reported in Figs. 4(a) and 4(b) for the as-grown (LCM1) and the fully oxygenated samples (LCM3). Similar maps have been obtained for the (103) asymmetric reflections. We infer that the as-grown film is fully tensile strained on the substrate, as shown by the same value of the Q_x position of the correspondent peaks in Fig. 4(a). This result is in agreement with the measurements reported by other authors.[24]

Because of the negative in-plane lattice mismatch between STO and LCMO, it is expected that a film of 300-Å thickness adapts itself to the substrate by increasing the values of the *a* and *b* axes. On the other hand, we have found that the oxygen annealing does not induce change in the *a*-*b* planes of the unit cells, as shown in Fig. 4(b), which are fully strained as in the as-grown film. The in-plane lattice parameters, a_F, reported in Table I, are calculated from the reciprocal space maps, while the *c*-axis lengths have been obtained from the spectra in Fig. 2. From the experimental data, it appears that the effect of the oxygen annealing is to increase the unit-cell volume by inducing an increase of the out-of-plane *c*-axis parameter leaving the $a-b$ lengths constant within experimental errors.

The effect of the oxygen annealing on the transport properties has been analyzed by means of the resistive measurements shown in Fig. 5. The samples show a metal-semiconductor transition with a temperature T_p, reported in Table I, which strongly depends on the oxygen content. The as-grown sample presents a transition temperature of 131 K, comparable to that measured by other authors in the case of

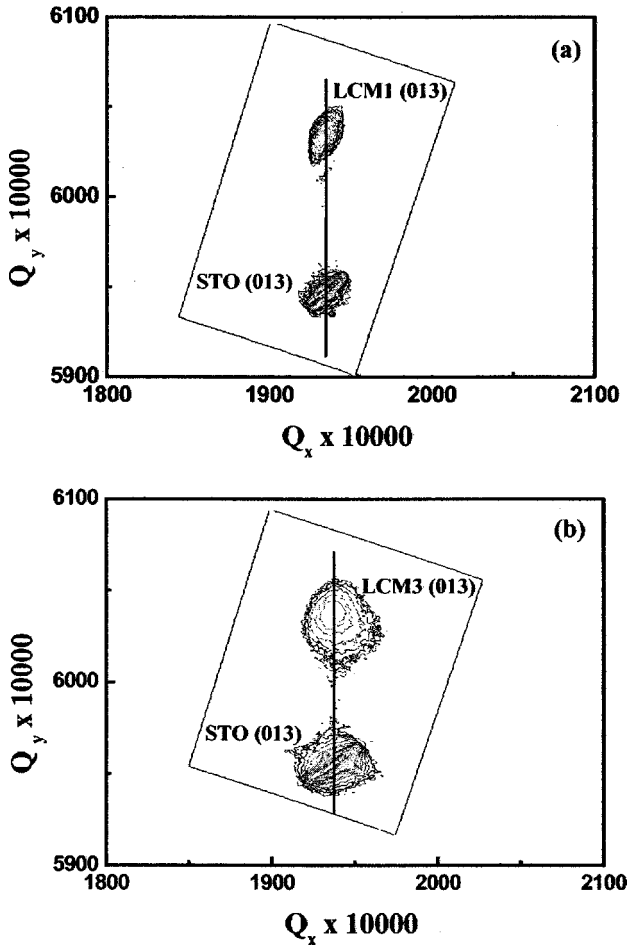

FIG. 4. Reciprocal space maps of the as-grown (a) and of the fully oxygenated (b) films. The maps show that both are fully strained on the substrates.

very thin LCMO films.[25] Increasing the annealing time, the film resistivity decreases while T_p increases up to 247 K for the fully oxygenated sample. Despite the increased structural disorder, the oxygen incorporation improves the transport properties. Indeed, as already observed in manganites, the transition temperature is strongly affected by the oxygen concentration rather than by the structural disorder.[26] Further

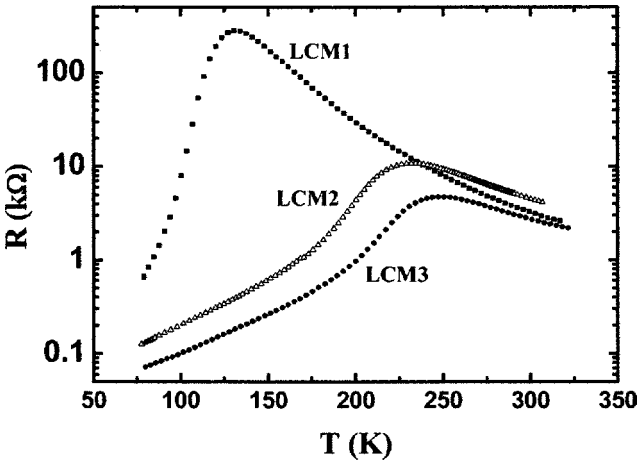

FIG. 5. Resistivity vs temperature data of the three samples. The T_p value, which corresponds to the maximum of the curve, increases with oxygen content.

oxygenation processes, both longer in time and higher in temperature, do not significantly improve T_p. Thus, according to other authors,[20] the LCM3 sample can be considered fully oxygenated with the highest metal-insulator transition temperature attainable in a 300-Å-thick film.

III. DISCUSSION

As reported by several authors, the metal-insulator transition can be driven by many physical mechanisms as hole doping,[1] orbital localization and charge-carriers density,[11] strain effects, and interstitial oxygen incorporation.[24] Our experimental results point out that the variation of T_p with the annealing procedure cannot be attributed to a unique phenomenon. Indeed, the increase of T_p can be explained by considering that the variation of the oxygen concentration leads to hole doping through an enhancement of the Mn^{4+}/Mn^{3+} ratio.[1,19] This effect can be quantitatively estimated considering that $Mn^{4+}/Mn^{3+}=h/(1-h)$, where $h=x+2\delta$ is the effective hole doping, and that $T_p \cong T_c = 2Ah(1-h)-Ah^2$ in a mean-field approximation, where A is a constant to be determined. The doping level depends on either the alkali ion and/or on the oxygen content. In our case, the measured Ca concentration is 0.3 in all the samples and the h variation is attributed only to the oxygen excess content 2δ. In the case of the fully oxygenated LCM3 sample, $2\delta=0$ and $h=x=0.3$ giving $A=748$ K. For the LCM1 sample, $T_p=131$ K and by considering the value obtained for the constant A, the mean-field approximation gives $h=0.104$ leading to $\delta=-0.1$. Considering the phase diagram of LCMO bulk and thin films,[1] the h value found above would give an insulating phase for our as-grown film while the resistivity versus temperature measurements shown in Fig. 5 clearly report a metallic behavior below $T_p=131$ K. This indicates that the strong variation of T_p observed in our samples cannot be only ascribed to a change in Mn^{4+} concentration.

In addition to this, the change of T_p in thin films can be also explained assuming a competition between the in-plane orbital localization and the rising of the in-plane charge-carriers density.[27] Following the double-exchange (DE) theory[28] for the charge transport in the a-b planes, the decrease in T_p is attributed to the localization of the $d_{x^2-y^2}$ orbitals, thus being a consequence of the change in the Mn–O–Mn bond angle. In the case of LCMO thin films deposited on STO, the orbital localization is enhanced by the tensile strain. According to the general elasticity theory, the tensile strain gives also rise to a reduction of the c-axis length with a consequent compression of the $d_{3z^2-x^2}$ orbital which causes an increase of the charge-carrier concentration in the a-b plane.[1] The consequent decrease or increase in T_b is related to the competition between orbital localization and in-plane charge-carriers enhancement. When the LCMO thin films are annealed, the oxygen atoms inserted in the lattice structure increase the Mn^{4+}/Mn^{3+} ratio, giving rise to a weakening of the stabilization of the $3z^2-r^2$ orbitals.[1] Therefore, the charge carriers added by the oxygen enrichment are incorporated in the $d_{x^2-y^2}$ orbitals, producing an increase of the carrier density in the a-b plane. Because no variation of the a-b lattice parameters is observed, the localization of the in-plane charge carriers results to be unchanged with respect to the as-grown sample and the net effect is an increase of T_p.

Moreover, the oxygen annealing also produces a change in the strain which induces a variation of T_p. On the other hand, the bulk compression tends to reduce the electron-lattice coupling, inducing an increase of T_p, while the biaxial strain reinforces the tendency of the electrons to become localized with a consequent decrease of T_p.[29] In Table I the bulk strain ε_B and the biaxial strain ε_{JT} (Ref. 13) are reported for the three different samples. Because the in-plane mismatch between the film and the substrate is fixed and does not depend on the annealing, the only contribution to the variations of ε_B and ε_{JT} comes from the c-axis elongation. As reported in Table I, the ratio $\varepsilon_B/\varepsilon_{JT}$ increases for the fully oxygenated film, providing an explanation for the strong increase observed in T_p. This is expected because the increase of the Mn^{4+} concentration reduces the Jahn–Teller (JT) effect and enhances the bulk term.

Finally, the oxygen incorporation within columns or grains of the film structure should also be taken into account.[24] In fact, the boundaries between columnar structures generated during the growth process can be filled by oxygen atoms, thus leading to a decrease of the resistivity. This mechanism can be considered as the main cause of the T_p enhancement in the case of films with thickness larger than 500 Å. However, the thickness and the structural quality of our films, as evidenced by the FWHM of the rocking curves and by the presence of satellite fringes, suggest that the oxygen incorporation between the grains is less effective than the above-mentioned mechanisms. This is supported by magnetoresisitivity measurements which for the fully oxygenated sample,[21] do not show any hysteresis as the direction of the applied magnetic field is inverted.

IV. CONCLUSIONS

In summary, we have shown that the oxygen postannealing in high-quality epitaxial LCMO thin films enhances the metal-insulator transition temperature by more than 100 K. In spite of the fact that the progressive annealing leaves the in-plane lattice parameters fully strained on the substrate, we have pointed out that the observed enhancement of T_p cannot be explained in terms of a unique underlying mechanism. Mn^{4+}/Mn^{3+} variation, hydrostatic, and Jahn–Teller distortion, as well as the possible inclusion of oxygen in the grain boundaries, should all be taken into account to consistently explain the experimental results.

[1] A. M. Haghiri-Gosnet and J. P. Renard, J. Phys. D **36**, R127 (2003).
[2] M. B. Salamon and M. Jaime, Rev. Mod. Phys. **73**, 583 (2001).
[3] H. Kawano, R. Rajimoto, M. Kubota, and H. Yoshizawa, Phys. Rev. B **53**, R14709 (1996).
[4] A. Urushibara, Y. Moritomo, T. Arima, A. Asamitsu, G. Kido, and Y. Tokura, Phys. Rev. B **51**, 14103 (1995).
[5] H. W. Zandbergen, S. Freisem, T. Nojima, and J. Aarts, Phys. Rev. B **60**, 10259 (1999).
[6] J. Aarts, S. Freisem, R. Hendrikx, and H. W. Zandbergen, Appl. Phys. Lett. **72**, 2975 (1998).
[7] S. Jacob, T. Roch, F. S. Razavi, G. M. Gross, and H.-U. Habermeier, J. Appl. Phys. **91**, 2232 (2002).
[8] S. Jin, T. H. Tiefel, M. McCormack, H. M. O'Bryan, L. H. Chen, R. Ramesh, and D. Schurig, Appl. Phys. Lett. **67**, 557 (1995).
[9] A. Biswas, M. Rajeswari, R. C. Srivastava, T. Venkatesan, R. L Greene, Q.

Lu, A. L. de Lozanne, and A. J. Millis, Phys. Rev. B **63**, 184424 (2001).
[10]T. K. Nath, R. A. Rao, D. Lavric, C. B. Eom, L. Wu, and F. Tsui, Appl. Phys. Lett. **74**, 1615 (1999).
[11]J. Zhang, H. Tanaka, T. Kanki, J. H. Choi, and T. Kawai, Phys. Rev. B **64**, 184404 (2001).
[12]J. Dho, Y. N. Kim, Y. S. Hwang, J. C. Kim, and N. H. Hur, Appl. Phys. Lett. **82**, 1434 (2003).
[13]F. Tsui, M. C. Smoak, T. K. Nath, and C. B. Eom, Appl. Phys. Lett. **76**, 2421 (2000).
[14]A. M. Haghiri-Gosnet *et al.*, J. Appl. Phys. **88**, 4257 (2000).
[15]R. Desfeux, S. Bailleul, A. Da Costa, W. Prellier, and A. M. Haghiri-Gosnet, Appl. Phys. Lett. **78**, 3681 (2001).
[16]O. I. Lebedev, G. Van Tendeloo, S. Amelinckx, B. Leibold, and H.-U. Habermeier, Phys. Rev. B **58**, 8065 (1998).
[17]R. A. Rao, D. Lavric, T. K. Nath, C. B. Eom, L. Wu, and F. Tsui, Appl. Phys. Lett. **73**, 3294 (1998).
[18]T. Y. Koo, S. H. Park, K. B. Lee, and Y. H. Jeong, Appl. Phys. Lett. **71**, 977 (1997).
[19]W. Prellier, M. Rajeswari, T. Venkatesan, and R. L. Greene, Appl. Phys. Lett. **75**, 1446 (1999).
[20]J. R. Sun, C. F. Yeung, K. Zhao, L. Z. Zhou, C. H. Leung, A. K. Wong, and B. G. Shen, Appl. Phys. Lett. **76**, 1164 (2000).
[21]A. De Santis, F. Bobba, G. Cristiani, A. Cucolo, K. Frohlich, H.-U. Habermeier, M. Salvato, and A. Vecchione, J. Magn. Magn. Mater. **211**, 41 (2003).
[22]L. G. Parrat, Phys. Rev. **95**, 359 (1954).
[23]L. Nevot and P. Croce, Rev. Phys. Appl. **15**, 761 (1980).
[24]S. Valencia, L. Balcells, J. Fontcuberta, and B. Martinez, Appl. Phys. Lett. **82**, 4531 (2003).
[25]M. Bibes, L. Balcells, S. Valencia, and J. Fontcuberta, Phys. Rev. Lett. **87**, 067210 (2001).
[26]B. C. Nam, W. S. Kim, H. S. Choi, J. C. Kim, N. H. Hur, I. S. Kim, and Y. K. Park, J. Phys. D **34**, 54 (2001).
[27]T. Kanki, H. Tanaka, and T. Kawai, Phys. Rev. B **64**, 224418 (2001).
[28]C. Zener, Phys. Rev. **81**, 440 (1951).
[29]A. J. Millis, T. Darling, and A. Migliori, J. Appl. Phys. **83**, 1588 (1998).